Kidney International, Vol. 63 (2003), pp. 1104–1115

Role of endogenous nitric oxide in unilateral ureteropelvic junction obstruction in children

Patricia G. Vallés, Luis Pascual, Walter Manucha, Liliana Carrizo, and Maria Rüttler

Cátedra de Fisiopatología, Facultad de Ciencias Médicas, Universidad Nacional de Cuyo and Hospital H. Notti, Mendoza, Argentina

Role of endogenous nitric oxide in unilateral ureteropelvic junction obstruction in children.

Background. Obstructive nephropathy leads to tubulointerstitial fibrosis and loss of renal function. Nitric oxide has been shown to have antifibrotic properties. We examined nitric oxide synthase (NOS) activity and expression in kidneys from children who underwent surgery release of unilateral ureteropelvic junction (UPJ) obstruction in relation to clinical and histologic parameters.

Methods. NOS activity and the expression of NOS isoforms measured at the mRNA level by reverse transcription-polymerase chain reaction (RT-PCR) assay were determined in tissue obtained by biopsy from obstructed kidneys of 18 children at the time of pyeloplasty. Tissue from kidneys removed because of various malignancies were issued as control.

Results. A significant increase in calcium/calmodulin-independent NOS activity (iNOS) and iNOS mRNA expression was found in the medulla of obstructed kidneys. Calcium/calmodulin-dependent NOS activity (cNOS) and endothelial (eNOS) mRNA, by contrast, were increased in the cortex from obstructed kidneys. A role of tumor necrosis factor-α (TNF-α) on enhanced iNOS was suggested by the finding of increased urine levels in obstructed pelvis. Increased interstitium macrophage number, by immunolabeling of CD68, was related to the delay in obstruction release and to decreased glomerular filtration rate (GFR) at surgery. A positive linear relationship was found between cNOS activity in cortex and creatinine clearance. The degree of interstitial fibrosis correlated negatively with cNOS activity in cortex.

Conclusion. In kidneys from children with UPJ obstruction an increased activity and expression of iNOS in medulla and cNOS-dependent eNOS in cortex were demonstrated. A role of cNOS in modulating GFR and interstitial fibrosis can be suggested. Prolonged UPJ obstruction would lead to a worsened prognosis on renal injury .

Key words: unilateral ureteropelvic junction obstruction, nitric oxide synthase activity, inducible nitric oxide synthase mRNA, tumor necrosis factor-α, macrophage, endothelial nitric oxide synthase mRNA.

Received for publication October 15, 2001
and in revised form October 24, 2002
Accepted for publication October 28, 2002

Congenital obstructive nephropathy is one of the primary causes of renal failure in infants and children [1]. The developing kidney is far more susceptible to injury resulting from chronic urinary obstruction in relation to adult kidneys. Whereas obstructive nephropathy in the adult is characterized by progressive interstitial infiltration by mononuclear cells, interstitial fibrosis and tubular atrophy, in the maturing kidney, impaired renal growth, and development are also included [2–3]. Interstitial macrophage kinetic data have shown that parenchymal infiltration develops 12 hours after ureteral ligation and significantly increases in the 3 days after obstruction [4]. The invasion of the renal interstitium by macrophages and T lymphocytes in experimental model of unilateral ureteral obstruction (UUO) coincides with a decline in renal hemodynamic parameters [5]. Decreased renal blood flow and glomerular filtration rate (GFR) in the unilateral obstructed kidney are mediated by several vasoconstrictors, including angiotensin II and tromboxane [6]. Following the onset of unilateral obstruction, angiotensin II production is rapidly stimulated [7]. Angiotensin II, in turn, up-regulates the expression of other factors, including tumor necrosis factor-α (TNF-α), a proinflammatory peptide produced by monocytes/macrophages and resident cells [8]. In human monocytic cell lines, the synergistic interaction between interferon-γ (INF-γ) and TNF-α in the expression of inducible nitric oxide synthase (iNOS) has been previously reported [9].

There is evidence that vasodilatory mechanisms respond to counterbalance renal vasoconstriction in obstruction. Besides, increased glomerular eicosanoid has been shown in UUO [10]. A role for soluble guanylyl cyclase to angiotensin-mediated vasoconstriction because of UUO has been reported [11].

Nitric oxide is also known to function as an antifibrotic factor in UUO [12]. Due to the interaction of nitric oxide and transforming growth factor-β (TGF-β) induced by angiotensin II, such may be a target for intervention in the fibrotic processes in obstruction [13]. We have demon-

strated interaction between angiotensin II and nitric oxide synthase (NOS) on the inhibition of H^+-ATPase in inner medullary collecting duct segments (IMCD) of experimental UUO kidneys [14].

Nitric oxide (NO) is a common but short-lived product derived from the amino acid L-arginine in a reaction catalized by a family of enzymes termed NOS, which convert arginine and oxygen into citrulline and NO [15]. The two major constitutive NOS isozymes, neuronal (nNOS) and endothelial (eNOS), exhibit strict dependency on intracellular calcium/calmodulin. Although they are classified as constitutive enzymes, expression of nNOS and eNOS is regulated by specific physiologic and pathophysiologic stimuli, including increases in local vascular resistance that enhances shear stress and hypoxia [16, 17]. The constitutive neuronal isozyme of NOS has been localized in the macula densa cells. By using reverse transcription-polymerase chain reaction (RT-PCR) of microdissected renal segments, Terada et al localized nNOS mRNA in IMCD segments and to a lesser extent, in the glomerulus and outer medullary collecting duct (OMCD) segments [18]. mRNA from eNOS has been demonstrated by RT-PCR in the glomerulus, preglomerular vasculature and in proximal tubules [19]. Expression of iNOS isoform has been demonstrated in epithelial cells of proximal tubules and IMCD tubules. Cytokines and lipopolysaccharides (LPS) induce the expression of iNOS [20].

Until now, NO synthesis by unilateral obstructed kidneys has been mainly demonstrated from experimental studies. This study was undertaken to examine the evidence for in vivo activity and expression of NOS isoforms in children with unilateral ureteropelvic junction obstruction (UPJO) and to suggest its clinical and histologic significance.

METHODS

Patients

This study protocol was approved by the Ethical Commitee of Notti Hospital and informed consent was obtained from all the children's parents after explaining the purpose of the study.

During the last 2 years, 18 patients [13 boys, age 2.41 ± 0.5 years (range, 7 months to 5 years) and five girls, age 5.28 ± 1 years (range, 5 months to 7 years)] with a diagnosis of UPJO (grade IV, hydronephrosis) and contralateral normal kidney operated on were studied. Initial screening for UPJO consisted of renal ultrasonography to evaluate hydronephrosis, according to the Society for Fetal Urology guidelines [21], and to measure the parenchyma thickness. A voiding cystourethrogram was performed in all cases to rule out vesicoureteral reflux. The diagnosis of obstruction was confirmed by technetium 99m-diethylenetriaminepentacetate acid (Tc 99m-DTPA) renal scan, which was performed using the standard protocols described by Majd [22]. All patients were hydrated with 5% dextrose in 0.3% sodium chloride (15 cm/kg) beginning 15 minutes before injection of the radionuclide. An in-dwelling bladder catheter was placed to maintain an empty bladder. The radionuclide, 0.1 μCi/kg Tc 99m-DTPA was administered as an intravenous bolus. Uptake of isotope between 1 and 3 minutes after radionuclide injection, with the region of interest outlined and background subtracted, was used to determine the percentage of contribution to total renal function of each kidney (differential renal function). When radionuclide activity in the hydronephrotic kidney and renal pelvis was observed to peak as monitored by the gamma camera, 1 mg/kg intravenous furosemide was given. The tracer activity corresponding to regions of interest over each kidney was observed for 30 minutes after the injection of furosemide. The reliability of the study has been demonstrated in neonates and infants [23].

Patients' weight and differential function for each kidney were recorded. Preoperative urinalysis and urine culture revealed sterile urine in all children. Before surgery, blood pressure was within normal limits [24]. Plasma creatinine showed normal values for their age [25].

Protocol

All patients underwent dismembered pyeloplasty. During the procedure, urine from obstructed kidney was obtained for the measurement of nitrite concentration, TNF-α levels, and creatinine excretion. A full-thickness biopsy was performed in the lower pole with a 10 Fr punch and a nephrostomy tube was placed in the corresponding calyx. Renal tissue was processed for microscopic optical analysis and stained through an immunoperoxidase method by using CD68 antihuman macrophage antibodies. The remaining renal tissue from each biopsy was frozen immediately and stored at −70°C until further analysis of NOS activity and NOS mRNA by RT-PCR. Owing to the small sample of tissue obtained at renal biopsy on the pediatric patients, both determinations could not been performed on the same sample. In 12 children, NOS activity was measured. NOS isoforms expression was performed on renal tissue samples from the remaining six patients.

Normal renal tissue was obtained from three patients in whom one kidney had been removed because of the presence of a carcinoma. None of the patients was on any drugs known to interfere with iNOS activity and expression at the time of biopsy. Renal biopsy was performed in all the children after parental informed consent had been obtained.

Seventy-two hours after the procedure and in the absence of hematuria, a 24-hour urine sampling was collected from nephrostomy tube and from uretra. Creatinine, electrolytes, ammonium, and titrable acid were measured. The next morning, the first urine samples from the catheter and from the uretra, under stream clean-

catch specimen, were divided into two aliquots, the first to measure urine osmolality and the second to freeze at −70°C for a later measurement of nitric oxide, TNF-α, and creatinine. No water deprivation challenge had been performed before the urine concentrating ability was tested.

A blood sample was obtained to measure creatinine, electrolytes, plasma osmolality, and arterial blood pH and pCO_2. GFR was measured by the endogenous creatinine clearance. Plasma and urine concentration of creatinine were determined using the modified Jaffe kinetic technique. Plasma and urine electrolytes were measured using an autoanalyzer.

Urine and plasma osmolality were assessed by Wescor Vapor Pressure Osmometer 5500 (Wescor, Inc., Logan, UT, USA). Urine ammonium was determined spectrophotometrically by the Berthelot (phenol-hypoclorite) reaction with minor modifications [26]. All standards (reagent grade NH_4Cl) and samples were prepared on the day of analysis. Ammonium analysis was performed immediately after collection. Interassay coefficient of variation was 6.2%. Titrable acid was measured by titulation. The results were expressed in μEq/min/1.73 m^2 corporal.

Urine nitrite concentration

Nitrite concentration in the urine was determined by the Griess reaction [27]. Nitrite reacts with 1 mmol/L sulfanilamide, 0.1 mol/L HCl/1 mmol/L naphthalene-ethylenediamine dihydrocloride (NED), forming a chromophore absorbing at 540 nm. The Griess reaction was performed immediately after receiving the samples. Urine samples (820 μL) and $NaNO_2$ and standards (10 to 100 μmol/L /1000 μL H_2O) were incubated at 37°C for 10 minutes with 40 μL sulfanilamide 1 mmol/L and 40 μL HCl 0.1 mmol/L. After 100 μL NED, 1 mmol/L was added and the samples were incubated at room temperature for 10 minutes. Absorbance was measured in a spectrophotometer at 540 nm.

Assay for cytokine TNF-α

Stored urine samples were thawed to room temperature before cytokine analysis. Samples were centrifuged at 3000 rpm for 10 minutes to remove cells and particulate matter. The supernatant was used. The urine profiles of TNF-α were determined by using the quantitative sandwich enzyme-linked immunosorbent assay (ELISA). Commercially available sandwich ELISA involves a monoclonal antibody coated to microtiter wells. Precise aliquots of the urine sample (200 μL) were added to each microtiter well coated with the appropriate cytokine antibody. The plate was covered with an adhesive strip to prevent sample evaporation. The apparatus was then incubated at room temperature for 2 hours. Each well was aspirated and washed after incubation for a total of three washes using an automated plate washer and wash buffer provided in the kit. Another horseradish peroxidase-conjugated polyclonal antibody (200 μL) directed against the cytokine was added, and the assay was incubated for 1 hour at room temperature. A stop solution was added and the optical density of each well was determined immediately on a dual wavelength ELISA reader at 450 nm and 570 nm, respectively, which corrects OD450 reading by subtracting OD570.

To allow the dilution effect of varying urine output, urinary levels of cytokines were expressed as the ratio of cytokine-to-urinary creatinine (pg/μmol).

Renal biopsy

All renal specimens processed for optical analysis were fixed in 10% buffered formalin, embedded in paraffin and stained with hematoxylin and eosin and masson tricromic. Two pathologists examined the biopsy material. Optical microscopic features in the glomeruli, tubules and interstitium were assessed regarding the severity of lesions. The extent of interstitial fibrosis was evaluated and graded on a percentage according to the lesion severity.

Immunohistochemical analysis

Kidney sections that had been fixed in 10% buffered formalin before being embedded in paraffin, were subsequently deparaffined and rehydrated and incubated with 3% H_2O_2 for 30 minutes to quench endogenous peroxidase activity. After washing in Tris-buffer pH 7.6 and nonspecific blocking with bovine serum albumin (BSA) 10% for 30 minutes, the sections were incubated with primary antibody 1:500 dilution of a CD68 mouse mAb (Dako Corporation, Carpinteria, CA, USA), at 4°C overnight. After being rinsed with phosphate-buffered saline (PBS), the sections were incubated with the secondary antibody, biotinylated rabbit polyclonal antibody against mouse antibody (Dako) for 60 minutes. The sections were then rinsed and incubated for 20 minutes with horseradish peroxidase–labeled streptavidin. Finally, sections were revealed with diaminobenzidine (DAB) kit (Dako) 1:25 in PBS plus 0.01% H_2O_2. After extensive washing in PBS, sections were counterstained with hematoxylin and examined under light microscopy. Positive controls run for each antibody (nodes sections) were processed. Negative controls were performed by omitting the primary antibody and employing a nonimmune mouse antiserum as first layer.

Quantitative study of CD68-positive cells

Interstitial macrophage infiltration was evaluated in the absence of any clinical data. Only cells with a clearly identifiable nucleus were counted. Positive cells were separately counted in a similar way as previously described [28], with some modifications. Briefly, in the cortex and medulla from randomly selected interstitial areas, CD68-

positive cells were counted by using an Ortholux (Ernest Leitz, Wetzlar, Germany) microscope eyepiece graticule to identify 10 adjacent, microscopic fields, each 0.046 mm^2. Hence, a total area of 0.46 mm^2 was counted. Macrophages were counted in the sequence of the aforementioned fields and no adjustments were made, except to avoid glomeruli and vessels. The numbers were expressed as CD68-positive cells per $mm^2 \pm$ standard error of the mean (SEM).

Renal tissue homogenates

Renal cortex and medulla were removed under a stereomicroscope. After weighing both, the cortex and the medulla were immediately frozen on dry ice. Later, the tissues were homogenized by using a glass homogenator (Lightnin Model Mixer-Volts 100, Mixing Equipment Co., Inc., Rochester, NY, USA) in a solution (10 mg tissue/100 μL solution) containing 10 mmol/L HEPES-Tris, 0.32 mol/L sacarose, 1 mmol/L DTT, 1 mg/100 mL soybean tripsin inhibitor, and 2.5 μg/mL trasylol to pH 7.40. The homogenate of each biopsy ($N = 12$) was used for the measurement of NOS enzyme activity. All chemicals were purchased from Sigma Chemical Company (St. Louis, MO, USA) unless otherwise noted.

Determination of nitrite release in homogenates from renal cortex tissue

We measured the release of nitrite on renal cortex tissue using a previously described method [29]. Homogenates from renal cortex tissue of obstructed kidneys and from tissue of cortex kidneys under nephrectomy issued as controls were incubated with 10 mmol/L L-arginine in a buffer (pH 7.40) containing 25 mmol/L HEPES, 140 mmol/L NaCl, 5.4 mmol/L KCl, 1.8 mmol/L $CaCl_2$, 1 mmol/L $MgCl_2$, and 5 mmol/L glucose at 37°C for 24 hours. After centrifugation at 6400 rpm for 20 minutes, the supernatants were used for the assay of NO production and the amount of NO_2^- was corrected by means of the protein amount, measured according to the Bradford method. Nitrite was measured by a spectrophotometer at 540 nm wavelength using the Griess reaction. The NO_2^- present was expressed as nanomole of nitrite generated per milligram of protein per minute.

Determination of NOS activity

NOS activity on renal homogenates of cortex and medulla was quantified by measuring the conversion of L-[^{3}H] arginine to L-[^{3}H] citrulline in the presence of saturating concentrations of the enzyme's cofactors as it was described before [30] with brief modifications.

Homogenates from renal biopsies were centrifuged at 3000 rpm at 4°C for 10 minutes. A 40 μL aliquot of the each supernantant fraction was incubated with 3 mmol/L $CaCl_2$, 1 mmol/L nicotinamide adenine dinucleotide phosphate (NADPH), 25 μmol/L flavin adenine dinucleotide (FAD), 1.25 μg/mL calmodulin, 10 μmol/L tetrahydrobiopterin, and L-[^{3}H] arginine (approximately 300,000 cpm, 6.8 Ci/mL) in 20 mmol/L HEPES buffer (reaction buffer), pH 7.40, at 37°C for 30 minutes. Calcium/calmodulin-independent NOS activity was measured by using the same buffer and cofactors, without calcium and calmodulin, after the addition of 0.5 mmol/L ethylenediaminetetraacetic acid (EDTA). Parallel reactions were analyzed in the presence of 20 mmol/L L-arginine analog *N*-nitro-L-arginine methyl ester (L-NAME), an inhibitor of inducible and constitutive isoforms of NOS in renal cortex and medulla of control kidneys. The reaction was stopped by the addition of L-NAME 20 mmolL HEPES buffer (100 μL) at 4°C. The total volume (210 μL) was applied to a Dowex 50W-X8, 100 to 200 mesh column (volume 0.6 mL) that had been preequilibrated with 20 mmol/L HEPES buffer (7.40) and saturated with 20 mmol/L cold citrulline. L-[^{3}H]citrulline was eluted with 200 μL deionized water and radioactivity was quantified by scintillation counting, (Wallac, LK Beta Rack, Finland). Blanks included 50 μL homogenate buffer plus 60 μL reaction buffer without or with calcium/calmodulin for measuring iNOS and cNOS, respectively. The results are expressed as fmol L-[^{3}H] citrulline/mg protein/minute incubation. Protein concentrations were measured according to Bradford [31] using Bio-Rad reagent (Richmond, CA, USA). BSA was used as standard (1 mg/mL).

RNA isolation, RT-PCR, and semiquantification for NOS isoforms

Total RNA was obtained from renal cortex and medulla by using Trizol reagent (Life Technologies, Gibco BRL, Gaithersburg, MD, USA). Three to five micrograms RNA have been denaturated in the presence of 0.5 μg/50 μL Oligo $(dT)_{15}$ primer and 40 U recombinant ribonuclease inhibitor (Rnasin, Promega, Madison, WI, USA). RT was performed in the presence of mixture using 200 U reverse transcriptase Moloney-murine leukemia virus (M-MLV) RT in reaction buffer (Promega), 0.5 mmol/L deoxynucleotide triphosphates (dNTPs) each and incubating 60 minutes at 37°C. The cDNA (10 μL) was amplified by PCR. Each sample from obstructed and control kidney cortex tissue was measured for iNOS, nNOS, eNOS, and β-actin cDNA in separate tubes by using 50 pmol from specific primers. iNOS expression was also performed in samples from obstructed and control kidney medullas. The upstream and downstream primers for iNOS were sense 5′-GCATGGACCAGT ATAAGGCAAGCA-3′ and antisense 5′-GCTTCTGG TCGATGTCATGAGCAA-3′, respectively. These yield a single band corresponding to a 220 bp fragment. Analysis of the sequence revealed that it was identical to position 1693-1915 in mouse macrophage iNOS cDNA [32].

The upstream and downstream primers for nNOS were 5′-GAACCCCCAAGACCATCC-3′ and 5′-TTGACAC

Table 1. Renal junction parameters 72 hours after obstruction release in children with unilateral ureteropelvic junction (UPJ) obstruction

Creatinine clearance *mL/min/1.73 m²*		Urine amonium *μEq/min/1.73 m²*		Titrable acid *μEq/min/1.73 m²*		Osmolality *mOsm/kg H_2O*	
OK	CLK	OK	CLK	OK	CLK	OK	CLK
16.4 ± 1.3[a]	50.1 ± 2.3	5.3 ± 0.9[a]	21.8 ± 3.0	4.7 ± 0.7[a]	23 ± 2.1	174 ± 17.2[a]	620.1 ± 63.7

Abbreviations are: OK, postobstructed kidney; CLK, contralateral kidney. Data are mean ± SEM.
[a] $P < 0.01$ OK vs. CLK

CCTCGTTTCGG-3′, respectively, which provide a single band encompassing the 308-bp cDNA fragment [33].

The upstream and downstream primers for eNOS (325 bp) were 5′-CTACAGAGCAGCAAATCCAC CCG-3′ and 5′-AGCAGTCGAAGGAGGCGAGGAC TAG-3′, respectively. These primers were designed by Dr Maria Rüttler using the PC/Gene (the nucleic acid and protein sequence analysis software system from the University of Geneva, Switzerland, IntelliGenetics Release 6.85, 1995, serial number IGI 3481).

The upstream and downstream primers for β-actin were sense 5′-TGGAGAAGAGCTATGAGCTGCCTG-3′ and antisense 5′-GTGCCACCAGACCAGCACTGTGTTG-3′, respectively, which yield a single band corresponding to a 201 bp cDNA fragment.

PCR was performed by incubating 10 μL sample cDNA with 50 mmol/L KCl Tris-ClH, 0.1% gelatin, 1.5 mmol/L $MgCl_2$, 2 U Taq polymerase, 0.2 mmol/L dNTPs, 50 pmol β-actin or iNOS, nNOS or eNOS primers in 50 μL final volume. PCR reaction was carried out for 30 cycles (30 seconds at 94°C; 60 seconds at 57°C, and 90 seconds at 72°C).

Relative quantification of NOS mRNA isoforms

The final PCR product (15 μL) was electrophoresed by using 2% agarose gel in Tris-borate disodium EDTA buffer. Gels were stained with 1 mg/mL ethidium bromide, visualized with an ultraviolet transluminator (UV Cole Parmer Instruments, Chicago, IL, USA), and photographed.

The photograph was digitized using a scanner (LACIE Silver Scanner for Macintosh) and the Desk Scan software (Adobe PhotoShop) on a desktop computer. The image was inverted before performing densitometric analysis using the United States National Institutes of Health Image 1.66 software (Rasband Wayne et al, Division of Computer Research and Technology, NIH, Bethesda, MD, USA). The NOS signal was standardized against β-actin signal for each sample and results were expressed as the NOS/β-actin ratio.

Statistical analysis

The results were assessed by one-way analysis of variance for comparisons between groups. Significance of differences was estimated by Bonferroni's test. Student *t* test was used to compare the means when the experimental design consisted of two samples. Statistical significance was assessed by Student impaired *t* test. Linear regression analysis was performed for the evaluation of the likelihood of cNOS or iNOS activity dependency on the GFR through the measurement of creatinine clearance in obstructed kidneys. Nonparametric correlation coefficient (Spearman *r* test) was performed pursuant to the relationship between the degree of interstitial fibrosis and the activity of nitric oxide synthase isoforms at renal cortex. $P < 0.05$ was considered to be significant. Results are given as means ± SEM. Statistical tests were performed by using GraphPad InSat version 3.00 for Windows 95 (GraphPad Software, Inc., San Diego, CA, USA).

RESULTS

Patients

Before surgery, 18 pediatric patients had a DTPA filtration rate difference of 36.0 ± 1.1%. Ultrasonography showed a parenchyma thickness in the obstructed kidney before surgery compared to normal kidney 3.7 ± 0.3 mm vs. 11.0 ± 0.3 mm ($P < 0.01$). Acid base balance was within normal range: pH 7.37 ± 0.02, pCO_2 (mm Hg), 36 ± 2, Hco_3^- (mEq/L), 21.2 ± 1.8. Table 1 shows data from glomerular and distal tubular function. Significant decrease of creatinine clearance (mL/min/1.73 m^2) was observed in the previously obstructed kidney (OK) related to contralateral kidney (CLK) ($P < 0.01$). The ability to concentrate the urine (mOsm/Kg H_2O) was impaired in OK compared to CLK ($P < 0.01$). An intensive defect on hydrogen ion secretion by the measurement of urine ammonium and titrable acid excretion (μEq/min/1.73 m^2) was observed on the previously OK compared to CLK.

Urinary levels of TNF-α (pg/μmol creatinine) showed a significant increase on pelvis urine after surgery, compared to the urine levels of the cytokine TNF-α obtained from bladder of the CLK ($N = 18$; 2.87 ± 0.27 vs. 0.17 ± 0.02 ($P < 0.01$). Significant differences were also demonstrated when urine levels of the cytokine TNF-α (pg/μmol creatinine) obtained from the nephrostomy tube of the previously OK was compared to urine cytokine levels of CLK bladder, 1.00 ± 0.19 vs. 0.17 ± 0.02 ($P < 0.05$) (Fig. 1). Pelvis urine nitrite (μmol/mL NO_2:μmol/mL creatinine) ($N = 18$) obtained during surgery significantly increased compared to nitrite urine

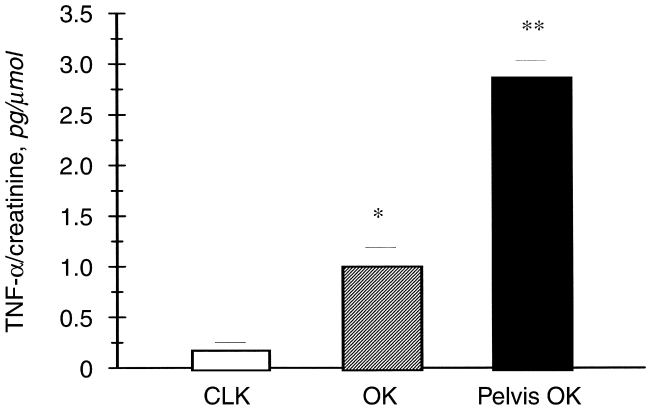

Fig. 1. Urinary levels of tumor necrosis factor-α (TNF-α). Urine from renal pelvis obtained during surgery proceeding pelvic obstructed kidney (Pelvis OK). Urine from obstructed kidneys (OKs) 72 hours after obstruction release. Urine from contralateral kidneys (CLK) 72 hours after obstruction release. Values are mean ± SEM ($N = 18$). *$P <$ 0.05 OK vs. CLK; **$P < 0.01$ pelvis OK vs. CLK.

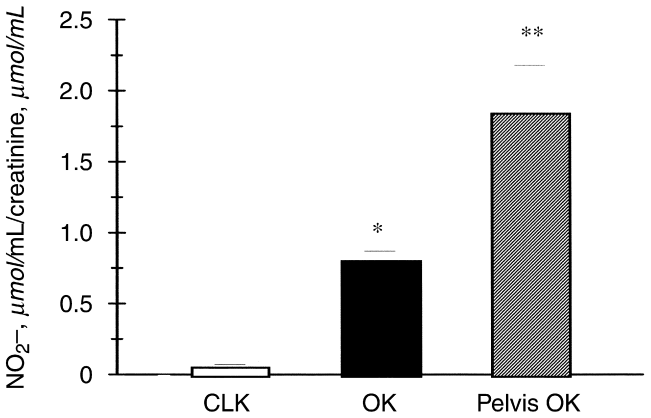

Fig. 2. Urinary nitrite concentration. Urine from renal pelvis obtained during surgery proceeding pelvic obstructed kidney (Pelvis OK). Urine from obstructed kidneys (Oks) 72 hours after obstruction release. Urine from contralateral kidneys (CLK) 72 hours after obstruction release. Values are mean ± SEM ($N = 18$). *$P < 0.05$ OK vs. CLK; **$P <$ 0.01 pelvis OK vs. CLK.

concentration obtained from bladder urine of CLK, 1.84 ± 0.33 vs. 0.04 ± 0.02 ($P < 0.01$). Minor differences were obtained on urine nitrite concentration (μmol/mL NO_2:μmol/mL creatinine) ($N = 18$), 72 hours after obstruction release; from the nephrostomy tube of the previously OK related to the nitrite urine concentration from the CLK bladder, 0.80 ± 0.07 vs. 0.04 ± 0.02 ($P <$ 0.05) (Fig. 2).

Immunochemical studies

Interstitial macrophage infiltration was detected by immunohistochemical staining for CD68 monoclonal antibodies. A significant increase in the cortical interstitium macrophage number, on CD68 immunolabeling, was shown between biopsies obtained from kidneys of children who underwent obstruction release at 1.2 ± 0.2 years of age ($N = 5$), and control kidney tissues: cortex, 47.8 ± 1.8 vs. 21.2 ± 1.5 CD68-positive cells/mm^2 ($P <$ 0.01).

By contrast, no differences were observed on renal interstitium medulla between these groups: 13.1 ± 6.2 vs. 11.6 ± 0.7 CD68-positive cells/mm^2. A significant difference in macrophage infiltration in cortex and medulla interstitium was found in kidney tissues from nine children who underwent obstruction release at 2.7 ± 2 years of age, compared to control kidney tissues ($N =$ 3): cortex, 419 ± 100 vs. 21.2 ± 1.5 CD68-positive cells/mm^2 ($P < 0.005$); medulla, 301.6 ± 55.3 vs./11.6 ± 0.7 CD68-positive cells/mm^2 ($P < 0.001$). In the OK tissue, the increased number of CD68-positive macrophage was observed in the peritubular cortical and medulla interstitial space. Immunocytochemical localization of CD68 also revealed that tubular epithelial cells from proximal tubules and cortical collecting ducts in cortex and dilated tubules at medulla showed CD68 expression within and on the cell surface in renal tissue from children who underwent delayed obstruction release, but not in controls (Fig. 3).

The Tc99m-DTPA renal scan and creatinine clearance study were performed in all patients ($N = 18$) at the time of renal biopsy to determine the relationship of the CD68-positive macrophage expression in the OK tissue and the renal hemodynamics. A significant decrease on GFR was observed in the group of children who presented the higher number of CD68-positive cells and who underwent obstruction release at 2.7 ± 2 years of age ($N = 9$), compared to the group of children who underwent obstruction release at 1.2 ± 0.2 years of age ($N = 5$) The Tc 99m-DTPA was 30.6 ± 1.3% vs. 36.1 ± 1.7% ($P < 0.05$), creatinine clearance (mL/min/1.73 m^2) was 13.21 ± 1.61 vs. 19.09 ± 2.17 ($P < 0.05$), respectively. However, two children under 8 months of age at the time of surgery who presented a severe decrease of GFR (<10 mL/min) were included in the group of increased number of interstitial macrophages.

No remarkable staining for CD68 was observed in OKs from four children with atrophia and intense fibrosis, released at mean 6.2 ± 0.1 years of age.

Nitrite oxide generated from renal tissue

Measurement of nitrite generated from homogenates of cortex tissue from OKs ($N = 6$) was significantly higher compared with the same tissue of control kidneys, 678.5 ± 121.3 vs. 330 ± 10 nmol/mg/min ($P < 0.05$).

NOS activity on renal tissue in obstruction

NOS activity was quantified by measuring the conversion of L-[^{3}H] arginine to L-[^{3}H] citrulline. When homoge-

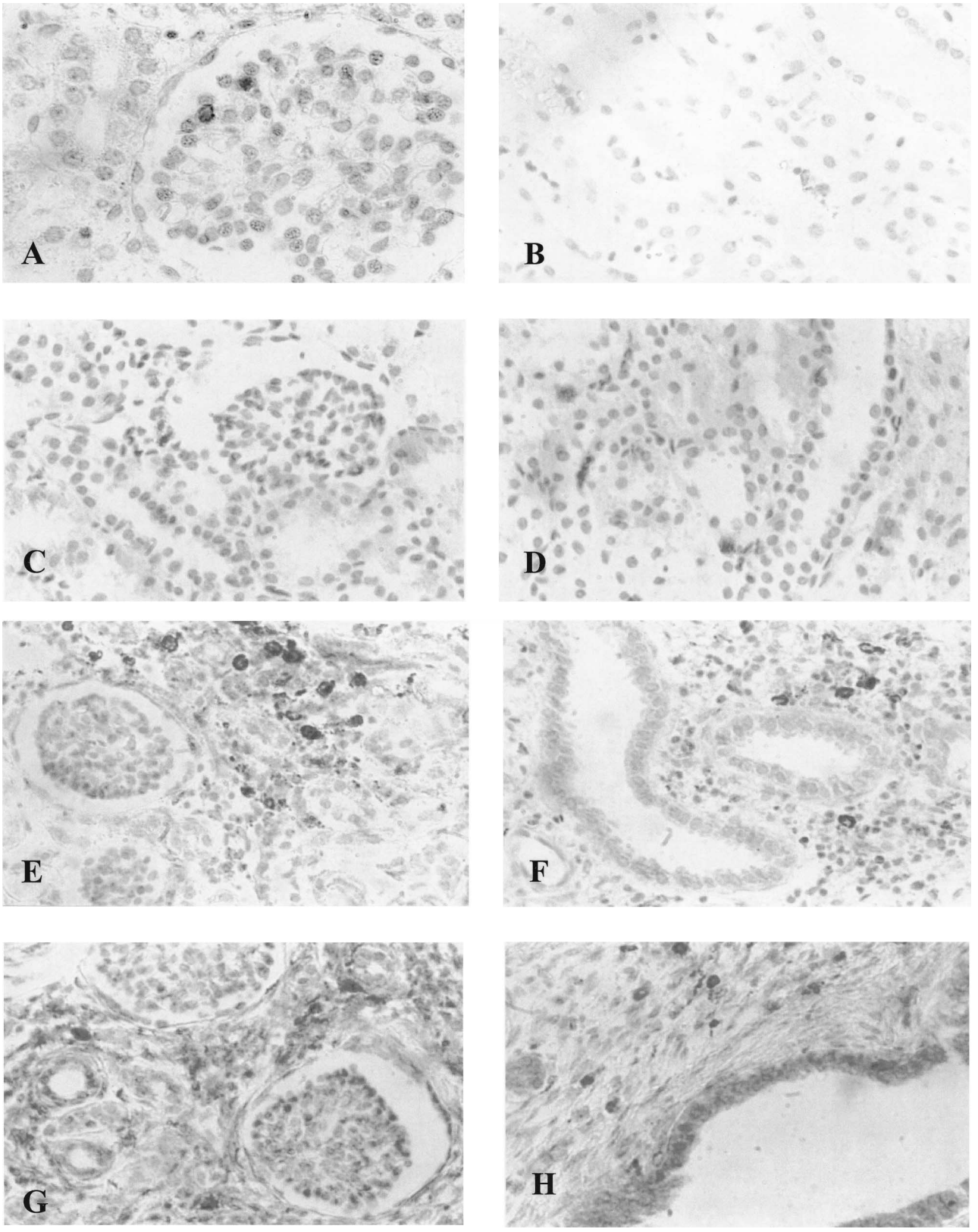

Fig. 3. Immunohistochemical staining for CD68 monoclonal antibodies. CD68 immunolabeling in tissue from control kidney. There is sparse interstitial macrophage infiltrate (×400). Immunostaining with CD68 antibodies of the cortex (*A*) and medulla (*B*) reveals a slight increase in macrophage interstitium infiltration on tissue from obstructed kidney in children who underwent obstruction release at 1 year of age. Immunostaining with CD68 antibodies of the cortex (*C*) and medulla (*D*) shows a higher increase in macrophage interstitium infiltration on tissue from obstructed kidney in children who underwent delayed obstruction release. Slight dilation of cortical collecting ducts and proximal tubules in the cortex (*E*). Intense dilation of medullary collecting ducts (*F*) with immunostaining with CD68 antibodies exhibits an intensive macrophage interstitium infiltration on tissue from obstructed kidney in children who underwent delayed obstruction release and intensive decrease on glomerular filtration rate (GFR) at surgery. CD68 expression within and on the cell surface in tubular epithelial cells from proximal tubules and cortical collecting ducts (*G*). CD68 expression within the cells in tubular epithelial cells from dilated medullary collecting ducts (*H*).

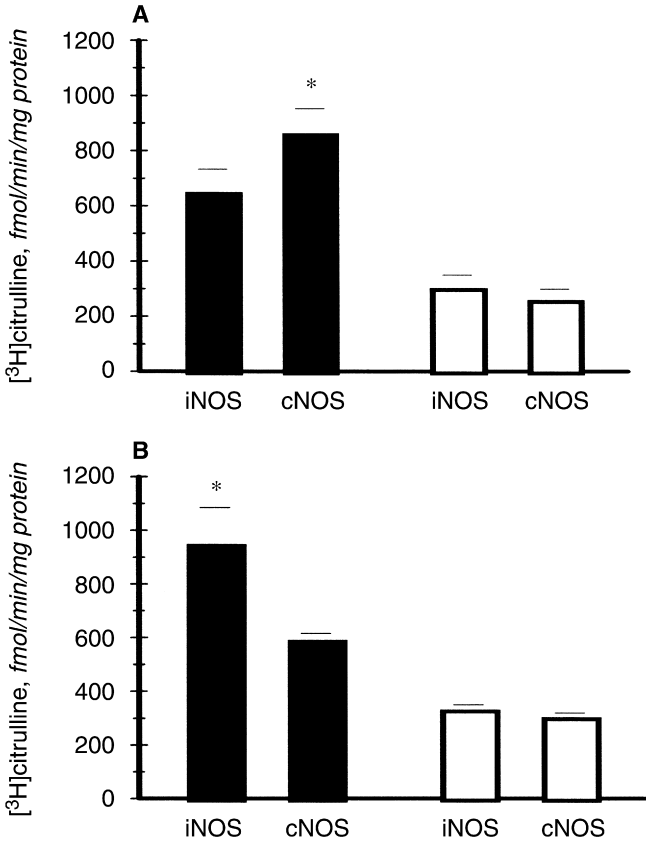

Fig. 4. Nitric oxide synthase (NOS) activity on tissues from obstructed kidneys and kidneys under nephrectomy. (*A*) Calcium/calmodulin-dependent NOS activity (cNOS) and calcium/calmodulin-independent NOS activity (iNOS) on tissue from cortex of obstructed kidneys (■) and on tissue from cortex of control kidneys (□). Values are mean ± SEM. *$P < 0.05$, cNOS on tissue from obstructed vs. control kidney cortex. (*B*) iNOS and cNOS on tissue from medulla of obstructed kidneys (■) and on tissue from medulla of control kidneys (□). Values are mean ± SEM. *$P < 0.05$, iNOS vs. cNOS on tissue from medulla of obstructed kidneys. *$P < 0.05$ iNOS on tissue from medulla of obstructed kidneys vs tissue from control kidney medulla.

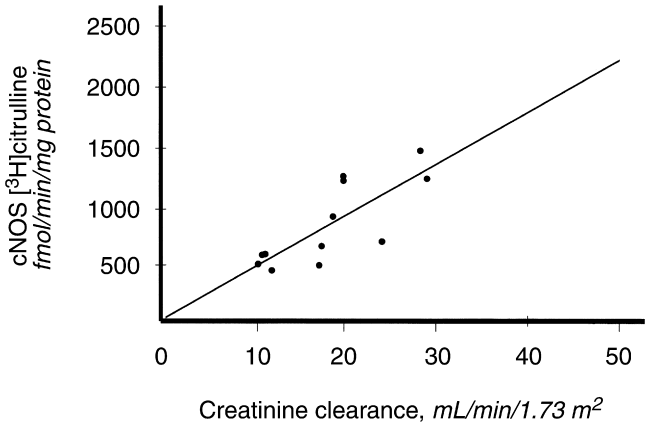

Fig. 5. Relationship between calcium/calmodulin-dependent NOS activity (cNOS) activity in cortex tissue from obstructed kidneys and glomerular filtration rate (GFR) through creatinine clearance in children with unilateral ureteropelvic junction (UPJ) obstruction 72 hours after surgery released. Symbols represent individual subjects. The solid line is the fitted, least squared, regression line. Y = 86.61 + 42.59 X; $r^2 = 0.61$; $P < 0.002$.

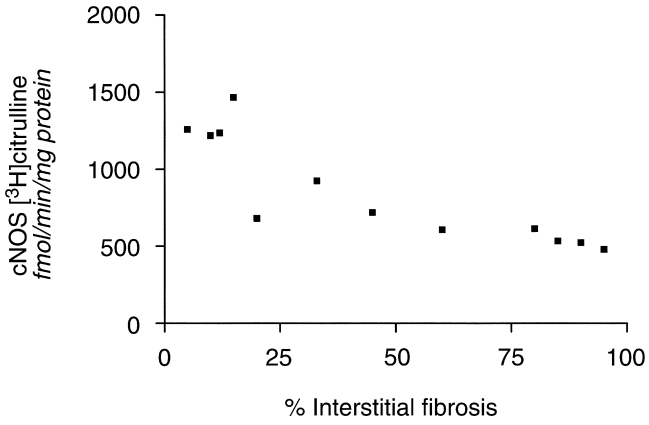

Fig. 6. Correlation in cortex tissue from obstructed kidneys between the calcium/calmodulin-dependent NOS activity (cNOS) activity and the severity of the tubulointerstitial damage evaluated through trichrome staining as a percentage. r = −0.92; $P < 0.001$.

nates from OK tissues ($N = 12$) were incubated in the presence of saturating concentrations of the enzyme cofactors, significant increase on cNOS activity (fmol L-[^{3}H] citrulline/min/mg protein) was observed in the cortex related to the cortex from control kidneys cNOS, 857.7 ± 96.2 vs. 253.1 ± 6.2 ($P < 0.05$). iNOS) (fmol L-[^{3}H]citrulline/min/mg protein) was observed in OK medulla tissues compared to control medulla tissues, 942 ± 143 vs. 325.2 ± 3.2 ($P < 0.05$). Significant increase on iNOS activity compared to cNOS activity was shown from OK medulla tissues, 942 ± 143 vs. 584 ± 32 ($P < 0.05$). On the contrary, no differences on cNOS activity compared to iNOS activity (fmol L-[^{3}H]citrulline/min/mg protein) were observed in OK cortex tissues, 857.7 ± 96.2 vs. 643.3 ± 90.2 (Fig. 4). The relationship between cNOS activity in renal cortex tissues and GFR 72 hours after obstruction release is depicted in Figure 5. The cNOS activity increased linearly in relation to GFR (r, 0.62; $P < 0.002$) (Fig. 5). Correlation between the cNOS activity in renal cortex tissue to the severity of the tubulointerstitial damage in renal cortex evaluated through trichrome staining is shown in Figure 6. Significant inversed correlation was shown (r, −0.92; $P < 0.001$). Interstitial fibrosis became severe according to the decrease in cNOS activity in the kidney homogenates. No correlation was observed between iNOS activity in cortex tissue of OKs and tubulointerstitial damage in tissue from OK cortex (r, 0.25; $P < 0.43$ NS).

NOS mRNA isoforms on renal tissue in obstruction

Under identical conditions, a constant amount from each sample of OK medulla and cortex ($N = 6$) and

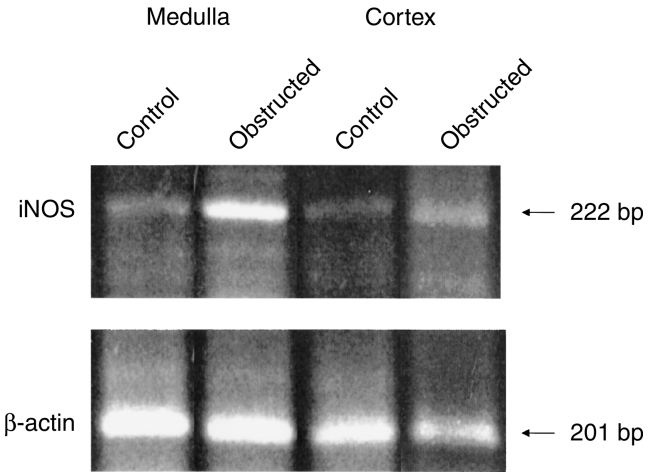

Fig. 7. Reverse transcription-polymerase chain reaction (RT-PCR) for inducible nitric oxide synthase (iNOS) and β-actin in human tissue from obstructed and control kidneys. PCR products from iNOS primers (220 bp) in human medulla and cortex tissues from control and obstructed kidneys. β-actin mRNA expression was also determined in RT-PCR on same samples. Ten microliters of the RT-PCR reaction were loaded on a 2% agarose gel and the DNA fragments were stained with ethidium bromide. These results are one of six independent observations.

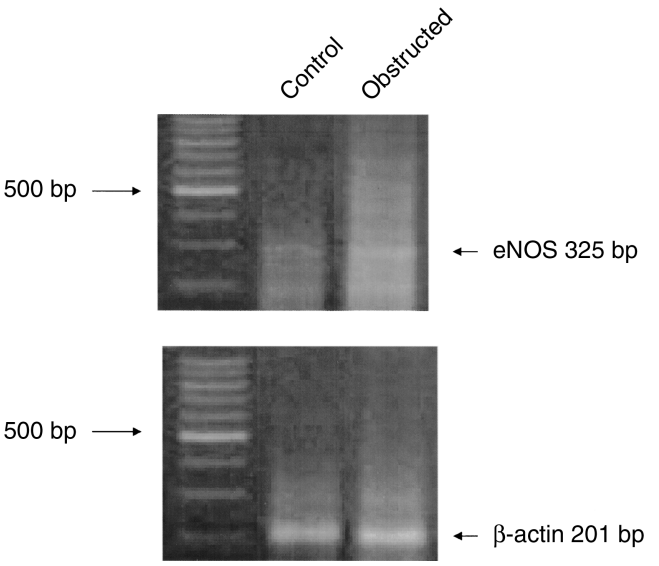

Fig. 8. Expression of endothelial nitric oxide synthase (eNOS) identified by reverse transcription-polymerase chain reaction (RT-PCR) in human cortex tissue from obstructed and control kidneys. Representative gel of PCR products from eNOS mRNA in control and obstructed human kidney cortex tissues. Amplification of the housekeeping β-actin cDNA (201 bp) from identical samples is shown. The first nonlettered lane represents the migration of 100 bp ladder of molecular weight standards from Promega, Madison, WI, USA. These results are one of six independent observations.

samples from control kidney medulla and cortex tissues ($N = 3$) were amplified by the PCR method and the integrated optical intensity of amplified target gene fluorescence in the ethidium bromide-stained were analyzed. The intensity of the amplified housekeeping gene, β-actin, was almost uniform in all tissues, confirming that the efficiency of RT did not vary significantly among samples. The target gene iNOS (220 bp) was clearly visible in obstructed kidney medulla and cortex tissues. A slight detection was demonstrated in control kidney cortex and medulla tissues. Densitometric analysis of the iNOS mRNA corrected for β-actin expression showed an increase in OK medulla compared to control medulla tissues (relative densitometric units), 0.753 ± 0.07% vs. 0.283 ± 0.01%, ($P < 0.01$). No significant difference was observed in OK cortex related to control renal cortex tissues, 0.499 ± 0.09 vs. 0.279 ± 0.05% (Fig. 7).

Increased eNOS mRNA corrected for β-actin mRNA was shown in cortex tissue from OKs compared to cortex from control kidneys (Fig. 8), with a densitometric ratio (relative densitometric units) of 0.885 ± 0.01% vs. 0.743 ± 0.03% ($P < 0.05$). The amplified gene nNOS against β-actin mRNA signal (relative densitometric units) showed no differences for cortex tissue of OKs compared to samples of control kidneys, nNOS, 0.602 ± 0.02% vs. 0.616 ± 0.03%.

DISCUSSION

NO is an important signaling and molecular mediator of essential biological processes. In the kidney, important actions of NO have been demonstrated, including regulation of glomerular hemodynamics and sodium and water excretion, as well as participation in both immune-mediated and hypoxia-reoxygenation–induced renal injury [17]. In the present study, presence of endogenous NO in renal tissue from unilateral UPJO was demonstrated through the enhanced in vivo iNOS and cNOS activity and increased iNOS and eNOS mRNA. To date, NOS by unilateral OKs has been mainly demonstrated from in vivo [34] and in vitro [12] experimental studies.

We demonstrated that there is in vivo induction of iNOS in human unilateral OK tissue. Both measurement of the iNOS activity and the iNOS expression through RT-PCR technique provided evidence for the existence of iNOS in renal tissue from children at the time of obstruction release. Enhanced iNOS expression and activity in tissue from OK medulla with lesser iNOS activity and expression on tissue from the OK cortex were shown. Conversely, increased cNOS activity and constitutive eNOS isoform mRNA were demonstrated in OK cortex tissues.The results of enhanced iNOS activity in renal medulla in obstruction are consistent with our previous data on an experimental model of UUO [14].

The regulation of iNOS expression and activity in response to inflammatory cytokines has been intensively communicated [20]. Recent evidence also suggests that iNOS may be constitutively expressed in the kidney [35]. Our results of the presence of basal activity and expres-

sion of the iNOS isoform in control kidney tissue confirm the constitutive expression and activity of iNOS. The increased expression of iNOS we detected from OK tissue is known to be induced by cytokines. Up-regulation of TNF-α has been reported in obstruction [8]. Binding to its receptors, TNF-α activates signals of transduction pathways that result in the expression of a variety of transcription factors, growth factors, and mediators of inflammatory processes [36]. The exposure to TNF-α, at medullary collecting duct cells in the kidney, induces expression of iNOS [20]. Experimental data support the concept that after unilateral obstruction of the kidney, TNF-α contributes to the increased macrophage migration into the renal interstitium of the affected kidney [37]. These data are consistent with the increased TNF-α excretion from urine of renal obstructed pelvis and enhanced interstitial macrophage infiltration that we have demonstrated in the patients. Furthermore, TNF-α has been found to stimulate the activity of a monocyte chemoattractant protein-1 (MCP-1), this chemokine has been proved to be a mediator of monocyte influx in the interstitium. Increased MCP-1 gene expression and urine excretion in congenital UPJO patients have been previously reported [38]. Thus, a role of TNF-α in the macrophage recruitment and deployment to the renal interstitium is suggested in children with UPJO. Despite a pattern that included a slight increase of macrophage in interstitial cortex, no significant differences were found in the expression of CD68-macrophage-positive cells between cortex and medulla interstitium in children with UPJO, by contrast to what had been previously described in an experimental model of obstructive nephropathy [4]. Our demonstration of immunocytochemical localization of CD68 in tubule epithelial cells of OKs could reveal macrophage infiltration on collecting tubules and dilated medullar tubules or that tubular epithelial cells exhibit sporadic CD68 expression within and on the cell surface. Morrissey et al [39] have described significant induction of CD14 mRNA in tubular epithelial cells in obstructed renal injury and its regulation by TNF-α through TNF receptor [39].

Presence of interstitial macrophage infiltration in this study showed that the increment in the number of CD68-macrophage-positive cells was related to the time of obstruction release and the initial obstruction severity through GFR. Sharp renal interstitial infiltration increment in the number of CD68-macrophage-positive cells was demonstrated in children who underwent delayed obstruction release. Notwithstanding two children, who were under 8 months of age at the time of surgery, were included in this group of increased number of interstitial macrophages. Those children had a marked decrease of GFR due to a severe obstruction degree. In like manner, experimental kinetics data had shown that interstitial macrophage number significantly increased as the obstruction time was lengthened [4]. The steady increase in the number of interstitial macrophages continuing to the decrease in renal function was noted due to the significant decrease in GFR and decreased filtration rate through renal scan in patients who underwent delayed obstruction release. Expansion of the interstitial volume that includes monocyte-macrophage infiltration leads to increased spatial separation of the peritubular capillary network from the tubules, resulting in insufficient perfusion and loss of transport efficiency [40]. Data of distal tubular function in the present study showed an intensely impaired hydrogen ion excretion in patients after kidney obstruction release. In accordance to these clinical results, we previously reported a significant decrease in H^+-ATPase activity on IMCDs in experimental UUO [41]. We demonstrated that endogenous NO increased by iNOS was involved in the inhibition of H^+-ATPase activity in obstructed IMCD segments [14]. A direct cytotoxic effect of high intratubular pressure in obstruction may be included in tubular hydrogen ion secretion defect and later progression to permanent renal injury. The loss of tubular epithelial cells leading to tubule atrophy has also been involved in renal function decline [42].

The role of infiltrating macrophages in decreasing GFR has been reported in obstructive nephropathy [5] Inflammation of renal interstitium may activate angiotensinogen transcription through cytokines [interleukin-1 (IL-1) and TNF-α] produced by macrophages or intrinsic renal cells [43]. Vasoconstrictors, including increased angiotensin II production, are known to mediate the selective increase in renal vascular resistance in the mechanism of reduced GFR in obstruction. Early on, after ureteral occlusion, an increase in glomerular capillary hydrostatic pressure, resulting in a lower net filtration pressure, has been shown in previous micropuncture studies [44]. Decreased renal flow, due to the constriction of the afferent arteriole, accompanied by a fall in plasma flow per nephron and decreased GFR, has been reported 24 hours after unilateral obstruction [2]. It is conceivable that physical stretch of the endothelium with an increased hydrostatic pressure enhances the release of endothelial-derived relaxing factor (EDRF) [34]. Although they are classified as constitutive enzymes, specific stimuli, including increased local vascular resistance and shear stress, have to be taken into account in obstruction.

Our present results showed increased cNOS activity in renal homogenates from obstructed cortex, with lesser activity on renal obstructed medulla. Modulation of renal hemodynamics by endogenous NO in response to intense vasoconstriction could be inferred from our results of the glomerular filtration effect on cNOS activity in obstruction. Participation of the eNOS isoform, localized to the renal endothelium of glomerular capillaries, afferent and efferent arterioles, in the modulation of renal vascular resistance could be demonstrated through our results

of increased eNOS mRNA expression by RT-PCR in the obstructed cortex.

Intrarenal vascular resistance adjustments include the tubuloglomerular feedback and the myogenic mechanisms. Presence of nNOS expression being localized to the cells of the macula densa by its contribution to the macula densa-dependent tubuloglomerular feedback signals participation in the regulation of glomerular ultrafiltration [45]. Increased nNOS could also be related to the increased renin secretion due to a lower NaCl delivery at macula densa pursuant to previous demonstration of abnormal sodium retention in obstruction [46]. Nonetheless, we could not demonstrate increased nNOS expression in OK cortex, related to control renal cortex as being involved in our results of increased cNOS activity.

NO not only modifies renal hemodynamics, but also fulfills the role of an antifibrotic factor in obstruction. The role of constitutive NOS in ameliorating interstitial fibrosis could be suggested due to the significant inverse correlation between cNOS activity and fibrosis degree in obstructed cortex kidneys. In an iNOS knockout mice model of unilateral obstruction, a significant role of eNOS has been shown for down-regulating renal fibrosis [47]. Loss of eNOS staining in peritubular capillaries of aging rats, contributing to increased tubulointerstitial renal injury, has also been reported [48]. In the present study, we provide evidence supporting the increased cNOS activity to be mainly related to eNOS isoform. A significantly higher eNOS expression was demonstrated through RT-PCR.

Previous support for iNOS-generating NO and its interaction with superoxide for peroxynitrite, a potent oxidant [49], includes the oxidative stress condition in the progression of tubulointerstitial injury in obstruction. In addition, iNOS knockout mice have been reported to be protected functionally and histologically from ischemia-reperfusion injury [50]. Notwithstanding, our results showed no correlation between iNOS activity in obstructed renal cortex and tubulointerstitial damage in tissue from OK cortex.

Owing to the interaction of angiotensin II and NO on renal fibrosis in obstruction, it has been demonstrated that angiotensin II and mechanical stretch stimulate NO expression in endothelial cells [49]. In a parallel way, angiotensin II and mechanical stretch induced TGF-β_1 expression involved in tubulointerstitial fibrosis obstruction in renal proximal tubule cells [13]. An interaction between NO and angiotensin II in the fibrotic process of children's upper urinary tract obstruction could be inferred based on a previous clinical study showing elevated bladder urine TGF-β_1 excretion [51] and our present data of enhanced nitrite excretion in the urine obtained from renal obstructed pelvis at the time of surgery, consistent with the NOS results.

Three days after KO release the urine nitrite concentration still showed higher urine concentration related to the one of the CLKs. The measured urinary nitrite was derived from NO generated by cNOS and iNOS. In the aftermath of a previous study, it was suggested that urinary nitrite excretion does not correlate with renal NO production [52]. Hence, we timely measured nitrite excretion from OK homogenates. A significant increase in NO release in obstructed renal homogenates was detected.

CONCLUSION

These results provide evidence for the increased cNOS activity and eNOS expression in the renal cortex, and iNOS activity and expression, likely induced by inflammatory cytokines at medulla tissue of unilateral UPJ obstructed kidneys in children.

Early cellular derangements showed increments in the number of CD68 macrophage-positive cells at interstitium, which are related to a late obstruction release and severity of the obstruction degree at time of surgery.

The role of endogenous NO through cNOS in modulating the intense vasoconstriction and fibrosis can be inferred from the increased cNOS activity in relation with enhanced GFR and decreased interstitial fibrosis. Prolonged UPJ obstruction would lead to a worsened prognosis on renal injury.

ACKNOWLEDGMENT

This work was performed with financial support from the Research and Technology Council of Cuyo University (CIUNC) from Mendoza, Argentina/N:631/99 to P.G.V.

Reprint requests to Patricia G. Vallés, M.D., Cátedra de Fisiopatología, Facultad de Ciencias Médicas, Universidad Nacional de Cuyo, Centro Universitario CP 5500, Mendoza, Argentina.
E-mail: pvalles@fmed2.uncu.edu.ar

REFERENCES

1. Warshaw BL, Edibrock HH, Ettenger RB: Progression to end stage renal disease in children with obstructive uropathy. *J Pediatr* 100:183–187, 1982
2. Chung KH, Chevalier RL: Arrested development of the neonatal kidney following chronic ureteral obstruction. *J Urol* 155:1139–1144, 1996
3. Chevalier RL, Chung KH, Smith CD, *et al*: Renal apoptosis and clusterin following ureteral obstruction: The role of maturation. *J Urol* 156:1474–1479, 1996
4. Diamond JR, Kees-Folts D, Ding G, *et al*: Macrophages, monocyte chemoatractant peptide-1 and TGFβ_1 in experimental hydronephrosis. *Am J Physiol* 266 (6 Pt 2):F926–F933, 1994
5. Harris KPG, Schreiner GF, Klahr S: Effect of leukocyte depletion on the function of the post-obstructed kidney in the rat. *Kidney Int* 36:210–215, 1989
6. Yarger WE, Schocken DD, Harris RH: Obstructive nephropathy in the rat: possible roles for the renin-angiotensin system, prostaglandins and tromboxanes in post-obstructive renal function. *J Clin Invest* 65:400–412, 1980
7. Pimentel JL, Martinez-Maldonado M, Wilcox JN, *et al*: Regulation of renin-angiotensin system in unilateral ureteral obstruction. *Kidney Int* 44:390–400, 1993
8. Kaneto H, Morrissey J, McCracken R, *et al*: The expression of

mRNA for tumor necrosis factor-α increases in the obstructed kidney of rats soon after unilateral ureteral ligation. *Nephrol* 2:161–166, 1996
9. Sanceau J, Wijdenes J, Revel M, *et al*: IL6 and IL6 receptor modulation by INF-γ and tumor necrosis factor-α in human monocytic cell line (THP-1). *J Immunol* 147:2630–2637, 1991
10. Yanagisawa H, Morrissey J, Morrison AR, Klahr S: Eicosanoid production by isolated glomeruli of rats with unilateral ureteral obstruction. *Kidney Int* 37:1528–1535, 1990
11. McDowell K, Chevalier R, Thornill B, Norling L: Unilateral ureteral obstruction increases glomerular soluble guanylyl-cyclase activity. *J Am Soc Nephrol* 6:1498–1503, 1995
12. Morrissey JJ, Ishidoya S, McCracken R, Klahr S: Nitric oxide generation ameliorates the tubulointerstitial fibrosis of obstructive nephropathy. *J Am Soc Nephrol* 7:2202–2212, 1996
13. Miyajina A, Chen J, Kirman I, *et al*: Interaction of nitric oxide and transforming growth factor-[beta] induced by angiotensin II and mechanical stretch in rat renal tubular epithelial cells. *J Urol* 164:1729–1734, 2000
14. Vallés P, Manucha W: H^+-ATPase activity on unilateral ureteral obstruction: Interaction of endogenous nitric oxide and angiotensin II. *Kidney Int* 58:1641–1651, 2000
15. Wang Y, Mursden PA: Nitric oxide synthases: Biochemical and molecular regulation. *Curr Opin Nephrol Hypertens* 4:12–22, 1995
16. Arnet UA, McMillan A, Dinerman JL, *et al*: Regulation of endothelial nitric oxide synthase during hypoxia. *J Biol Chem* 27:15069–15073, 1996
17. Kone BC, Baylis C: Biosynthesis and homeostatic roles of nitric oxide in the normal kidney. *Am J Physiol* 272 *(Renal Physiol* 41):F561–F578, 1997
18. Terada Y, Tomita K, Nonoguchi H, Marumo F: Polymerase chain reaction localization of constitutive nitric oxide synthase and soluble cyclase messenger RNAs in microdissected rat nephron segments. *J Clin Invest* 90:659–665, 1992
19. Ujiie K, Yuen J, Hogarth L, *et al*: Localization and regulation of endothelial NO synthase mRNA expression in rat kidney. *Am J Physiol* 267 (2 Pt 2):F296–F302, 1994
20. Markewitz BA, Michael JR, Kohan DE: Cytokine-induced expression of a nitric oxide synthase in rat renal tubule cells. *J Clin Invest* 91:2138–2143, 1993
21. Maizels M, Reisman ME, Nelson J, *et al*: Grading nephroureteral dilatation detected in the first year of life. Correlation with obstruction. *J Urol* 148 (2 Pt 2):609–614, 1992
22. Majd M: Nuclear medicine in pediatric urology, in *Clinical Pediatric Urology, 3rd ed.*, edited by Kelalis P, King LR, Belman AB, Philadelphia, WB Saunders Co, 1992, pp 117–165
23. Chung S, Majd M, Gil Rushton H, Belman B: Diuretic renography in the evaluation of neonatal hydronephrosis: is it reliable? *J Urol* 150:765–768, 1993
24. Report of the Second Task Force on Blood Pressure Control in Children: From the Natural Heart, Lung and Blood Institute, Bethesda, MD: *Pediatr* 79:1–20, 1987
25. Schwartz GJ, Haycock GB, Spitzer A: Plasma creatinine and urea concentration in children. *J Pediatr* 88:828–832, 1976
26. Cunarro J, Weiner M: A comparison of methods for measuring ammonium. *Kidney Int* 5:303–305, 1974
27. Griess JP: On a new series of bodies in which nitrogen is substituted for hydrogen. *Phil Trans R Soc Lond* 154:667–731, 1864
28. Alexopoulos E, Seron D, Hartley RB, *et al*: The role of interstitial infiltrates in IgA nephropathy: A study with monoclonal antibodies. *Nephrol Dial Transplant* 4:187–195, 1989
29. Tojo A, Kobayashi N, Kimura K, *et al*: Effects of antihypertensive drugs on nitric oxide synthase activity in the rat kidney. *Kidney Int* 49 (Suppl 55):S138–S140, 1996
30. Bredt DS, Synder SH: Nitric oxide mediates glutamate-linked enhancement of cGMP levels in the cerebellum. *Proc Natl Acad Sci USA* 86:9030–9033, 1989
31. Bradford MM: A rapid and sensitive method for the quantification of microgram quantities of protein utilizing the principle of protein-dye binding. *Anal Biochem* 72:248–254, 1976
32. Lyons CR, Orloff GJ, Cunningham JM: Molecular cloning and functional expression of an inducible nitric oxide synthase from a murine macrophage cell line. *J Biol Chem* 267:6370–6374, 1992
33. Bobadilla NA, Tapia E, Jimenez F, *et al*: Dexamethasone increases eNOS gene expression and prevents renal vasoconstriction induced by cyclosporin. *Am J Physiol* 277 (*Renal Physiol* 46): F464–F471, 1999.
34. Lanzone JA, Gulmi FA, Chou SY, *et al*: Renal hemodynamics in acute unilateral obstruction: Contribution of endothelium-derived relaxing factor. *J Urol* 153(6):2055–2059, 1995
35. Ahn K, Mohaupy M, Madsen KM, Kone BC: In situ hybridization of mRNA encoding inducible nitric oxide synthase in rat kidney. *Am J Physiol* 267 (5 Pt 2): F748–757, 1994.
36. Ortiz A, Bustos C, Alcazar A, *et al*: Involvement of tumor necrosis factor α in the pathogenesis of experimental and human glomerulonephritis, in *Advances in Nephrology*, edited by Grunfeld JP, Bach JF, Kreis H, Maxwell MH, St Louis, Mosby, pp 53–77, 1995.
37. Klahr S, Morrissey J: The role of growth factors, cytokines, and vasoactive compounds in obstructive nephropathy. *Semin Nephrol* Vol 18 (No 6):622–632, 1998
38. Grandaliano G, Gesualdo L, Bartoli F, *et al*: MCP-1 and EGF renal expression and urine excretion in human congenital obstructive nephropathy. *Kidney Int* 58:182–192, 2000
30. Morrissey J, Guo G, Mccracken R, *et al*: Induction of CD14 in tubular epithelial cells during kidney disease. *J Am Soc Nephrol* 1:1681–1690, 2000
40. Ishidoya S, Morrissey J, Cracken R, Klahr S: Delayed treatment with enalapril halts tubulointerstitial fibrosis in rats with obstructive nephropathy. *Kidney Int* 49:1110–1119, 1996
41. Vallés P, Merlo V, Berón W, Manucha W: Recovery of distal nephron enzyme activity after release of unilateral ureteral obstruction. *J Urol* 161:641–648, 1998
42. Truong LD, Sheikh-Hamad D, Chakraborty S, Suki WN: Cell apoptosis and proliferation in obstructive uropathy. *Semin Nephrol* 18:641–651, 1998
43. Brasier AR, Li J, Wimbish KA: Tumor necrosis factor activates angiotensinogen gene expression by the Rel A transactivator. *Hypertens* 27:1009–1017, 1996
44. Ichikawa I: Evidence for altered glomerular hemodynamics during acute nephron obstruction. *Am J Physiol* 82:F580–F585, 1982
45. Ichihara A, Navar G: Neuronal NOS contributes to biphasic autoregulatory response during enhances TGF activity. *Am J Physiol* 277 (*Renal Physiol* 46):F113–F120, 1999
46. Yarger WE, Buerkert J: Effect of urinary tract obstruction on renal tubular function. *Semin Nephrol* 2:17–30, 1982
47. Huang A, Palmer L, Hom D, *et al*: The role of nitric oxide in obstructive nephropathy. *J Urol* 163:1276–1281, 2000
48. Thomas SE, Anderson S, Gordon KL, *et al*: Tubulointerstitial disease in aging: evidence for underlying peritubular capillary damage, a potential role for renal ischemia *J Am Soc Nephrol* 9:231–242, 1998
49. Pueyo ME, Arnal JF, Rami J, Michel JB: Angiotensin II stimulates the production of NO and peroxynitrite in endothelial cells. *Am J Physiol* 274 (*Cell Physiol* 43):C214–C220, 1998
50. Ling H, Edelstein CH, Gengaro P, *et al*: Attenation of renal ischemia-reperfusion injury in inducible nitric oxide synthase knockout mice. *Am J Physiol* 277 (*Renal Physiol* 46):F383–F390, 1999
51. Furness PD, Maizels M, Won Han S, *et al*: Elevated bladder urine concentration of transforming growth factor β_1 correlates with upper urinary tract obstruction in children. *J Urol* 162:1033–1036, 1999
52. Sever R, Cook T, Cattell V: Urinary excretion of nitrite and nitrate in experimental glomerulonephritis reflects systemic immune activation and not glomerular synthesis. *Clin Exp Immunol* 90:326–329, 1992